Pergamon

PII: S0042-6989(97)00126-0

Vision Res., Vol. 37, No. 23, pp. 3273–3282, 1997

Printed in Great Britain
0042-6989/97 $17.00 + 0.00

Texture Density Aftereffects in the Perception of Artificial and Natural Textures

FRANK H. DURGIN,*† ALEXANDER C. HUK*

Received 29 October 1996; in revised form 18 April 1997

Three experiments are reported concerning the texture density aftereffect. The experiments address the question of how visual texture density information is encoded by examining patterns of transfer between different textures. In the first two experiments, it is shown that manipulation of spatial frequency and orientation information does not affect the *direction* of the aftereffect of density (reduction in perceived density), though similarity between adaptation and test textures does influence aftereffect *strength*. The third experiment demonstrates that adaptation to density differences in artificial textures in which spatial frequency information is held constant produces density aftereffects in naturalistic test textures in which density and spatial frequency covary.

Texture Adaptation Aftereffect Density Spatial frequency

INTRODUCTION

MacKay (1964) reported a kind of perceptual distortion in which the perceived grain of a sandpaper-like texture became coarse after extended viewing. Walker (1966) explored a variant of this as a texture density aftereffect, but Anstis (1974) suggested that the density aftereffect could be subsumed by the spatial-frequency-shift aftereffect (Blakemore & Sutton, 1969). To support this idea, Anstis adapted observers to textures which were different magnifications of sandpaper, typed text or gratings. He showed that perceptual size/density distortions occurred which were consistent with the spatial frequency-shift aftereffect. These aftereffects could be obtained between different types of texture in a manner predictable from spatial frequency coding (e.g. Blakemore & Campbell, 1969; Graham, 1989).

Durgin and Proffitt (1991, 1996); Durgin (1996a,b) have used balanced-dot (Carlson, Moeller & Anderson, 1984; Carlson *et al.*, 1984; Gilden, Bertenthal & Othman, 1990) textures in which element magnification (and thus spatial frequency) did not covary with density in order to demonstrate versions of texture density aftereffects for which a spatial-frequency shift account seems less plausible (cf. also, Durgin, 1995). Specifically, they have argued that density is not coded in the magnitude spectrum of a Fourier Analysis, and that a true density aftereffect can occur by the adaptation of information which is not specified in the frequency domain. Earlier studies (i.e. Anstis, 1974; Walker, 1966) had used textures for which density and spatial frequency covaried. A version of the density aftereffect in which density and spatial frequency do not covary is demonstrated in Fig. 1 (after Durgin & Proffitt, 1991).

By producing textures for which density and spatial frequency did not covary, Durgin and Proffitt (1991, 1996) sought to isolate density adaptation. However, because the density aftereffects they demonstrated are expressed as a local reduction in perceived density (an increase in perceived spacing), and the dots used were small, it remains possible that the dense balanced-dot textures employed by Durgin and Proffitt (1996) produced a shift in spatial frequency sensitivity away from the high spatial frequencies of the dots themselves. Thus, in practice, the visual system might have confounded Fourier size and density coding and produced these aftereffects despite the theoretical separability of spatial frequency and texture density.

The present experiments are designed to more directly test the relationship between spatial frequency information and density aftereffects. We will do this by varying the spatial-frequency content of the adaptation and test textures in order to determine the extent to which density adaptation is specific to the orientations and spatial frequencies of the adapting textures (Experiments 1A and 1B), and whether a spatial-frequency shift account remains viable as the spatial frequencies of the adaptation textures are manipulated (Experiment 2). Furthermore we will demonstrate that this kind of non-Fourier density adaptation also has measurable effects on naturalistic textures (Experiment 3).

At a descriptive level, density adaptation produces an

*Department of Psychology, Swarthmore College, 500 College Avenue Swarthmore, PA 19081, U.S.A.
†To whom all correspondence should be addressed [*Tel.*: 610 328 8678; *Fax*: 610 328-7814; *Email*: fdurgin1@swarthmore.edu].

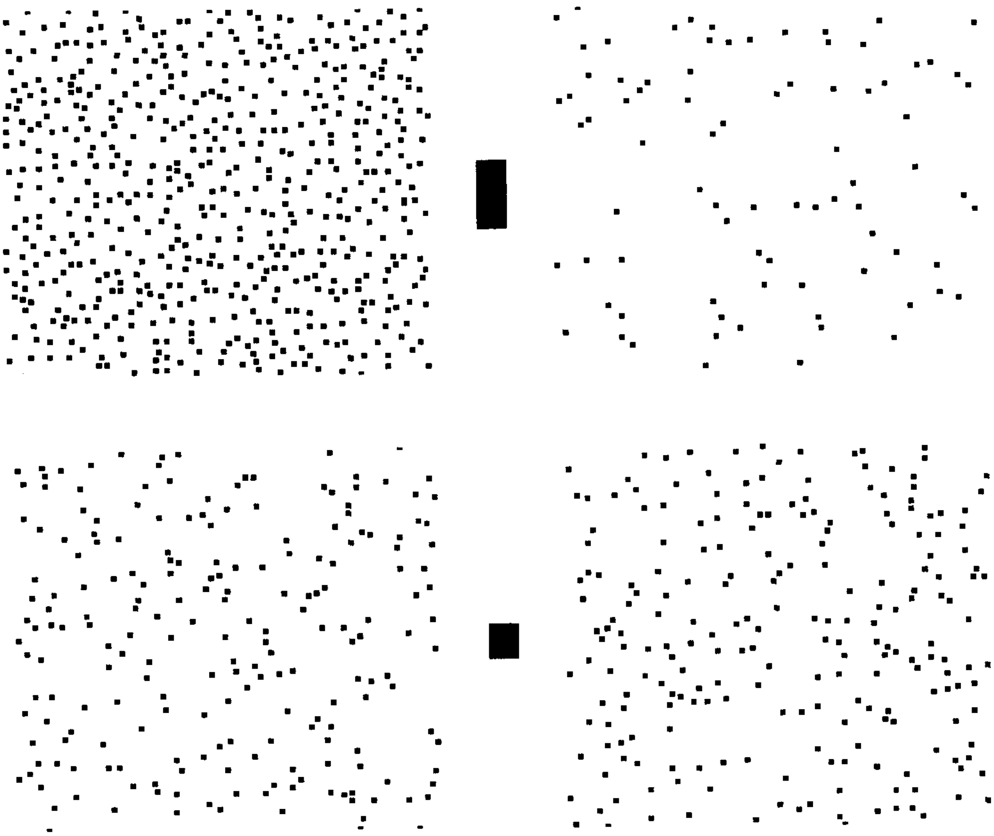

FIGURE 1. Stimulus for generating and observing a density aftereffect with constant-size elements. After gazing at the upper fixation mark for 15 or 30 sec, inspection of the lower texture pair while gazing at the lower fixation mark will result in a strong distortion of perceived density. Note that some distortion from simultaneous density contrast (Durgin and Proffitt, 1991) may be evident in the figure even prior to adaptation. Luminance confounds can be avoided by using luminance-balanced dots for elements.

apparent repulsion of elements. This repulsion effect may be related to the figural aftereffects studied by Köhler and Wallach (1944); cf. also, Gibson (1933). They demonstrated a kind of contour repulsion effect in vision for which they proposed a physical field mechanism. Without wishing to commit ourselves to their improbable neural physics, we believe that the notion of local spatial repulsion provides a good description of the density aftereffect though we doubt that the underlying representation is much more complicated than a scalar value. Although the change in the underlying perceptual representation is probably much more abstract than the distortion of absolute element position, we suggest that density aftereffects occur in the space domain, not the frequency domain.

EXPERIMENT 1A

Two-dimensional spatial-frequency coding includes information about both size and orientation. The spatial frequency information in a randomly-scattered texture can be manipulated by changing the spatial frequency content of the texture elements. In this experiment we used textures made up of small Gabor patches because the size and density of the Gabor patches could be maintained across experimental conditions while their orientation and spatial frequency was varied. Using textures composed of oriented bars, Durgin and Proffitt (1996) have shown that texture density aftereffects show some texture-element specificity, though the goals and design of that experiment were quite different from the present one. It is our present goal to examine the extent to which aftereffects generated by textures of one type transfer to textures of another.

Note that if the spatial-frequency shift aftereffect is responsible for density aftereffects, then adaptation to low-spatial frequency textures ought to *increase* the perceived density of higher spatial frequency textures (contrary to the normal density aftereffect). As will be shown below, this prediction fails. On the other hand, some modulation of the measured density aftereffect may be accounted for by similarities between the spatial-frequency of the test and adapting textures.

Method

Observers were adapted to differences in density between two regions and then tested for aftereffects to eight kinds of texture. Test textures could differ from the adaptation texture in the spatial frequency and/or the orientation of their elements.

Observers. There were eight observers. Two were the authors. The other six were Swarthmore undergraduates who were naive to the purpose of the experiment. Each observer participated in two adaptation sessions which differed in the spatial frequency of the adaptation texture.

Apparatus. The displays were generated and displayed using a Power Macintosh 9500/120 with a Javelin 3200 PCI video card which allowed a 1600×1200 pixel resolution on a Viewsonic 17" multisync monitor at a vertical refresh of 66 Hz. At the viewing distance of 54 cm, the horizontal and vertical resolution of the screen was 50 pixels per degree of visual angle. The mean luminance of the display was 35 cd/m^2. The experimental room was darkened.

Textures. Texture elements were odd-symmetric Gabor patches with spatial frequencies of either 2.5 or 5 c/deg. The sinusoids were windowed in a circular Gaussian window ($SD = 0.13$ deg) truncated at a radius of 16 pixels (2.5 standard deviations). Although the relatively small window size reduces orientation specificity of the Gabors, it facilitated the dense non-overlapping scatter of texture. Peak contrast [(Max − Min)/(Max + Min)] was nominally 100% to maximize adaptation. To avoid luminance artifacts associated with horizontal inter-dependencies on a raster monitor, oblique orientations were employed in Experiment 1A. (The monitor was physically rotated by 45 deg in Experiment 1B so that horizontal and vertical orientations could also be tested.) All four oblique orientations of each size texture were tested, with the result that Gabors differing by 180° actually differed in phase rather than orientation. These phase differences were perceptually salient for the 2.5 c/deg Gabors (for which only ca 1 cycle was visible).

Textures were displayed to the left and right of fixation in regions 15 deg $\times$ 22 deg (display duration was always 758 msec). The two regions were separated horizontally by 1°. Each texture was composed of some number of a single kind of element which was scattered randomly (with the constraint that elements did not overlap). New textures were generated for each trial. The dense adapting textures contained 400 elements, meaning *ca* 1.2 elements per square degree of visual area. The textured area was therefore roughly 40% "filled" with texture material (assuming an element radius of 16 pixels). Sparse adapting textures contained 50 elements (0.15 elements per square degree; 5% filled).

Adaptation. Observers maintained fixation while adapting texture pairs were displayed. Each pair consisted of a dense adapting texture presented on one side of fixation and a sparse adapting texture presented to the other side. We will refer to the dense-adapted side as the *adapted region* because the sparse adapting textures have little perceptual consequence, and are mainly included to maintain texture and contrast processing in the *unadapted region.* The side of the adapted region differed between observers. An initial sequence of 120 pairs of adapting textures (each texture newly generated) was presented with an ISI of 758 msec. Prior to each measurement trial, two further readapting texture pairs were presented to maintain the effect strength (cf. Durgin, 1995; Durgin & Proffitt, 1996). Each observer was adapted on one occasion to the high-spatial-frequency textures and on another occasion to a low-spatial-frequency texture.

Measurement. The modified staircase method we used for measuring the density aftereffect is described in detail elsewhere (e.g. Durgin, 1995; Durgin & Proffitt, 1996). In brief, eight interleaved staircases were used to estimate points of subjective equality (PSE) for textures presented concurrently in the adapted and unadapted regions. One staircase was used for each kind of Gabor texture defined as a $2 \times 2 \times 2$ combination of orientation (45 or 135 deg), phase (0 or 180 deg) and spatial frequency (2.5 or 5 c/deg). Staircases began at objective equality (unbeknownst to the naive observers), using a standard density in the adapted region that was half of the adapting density (i.e. 200 Gabors). The variable field (the identity of which was not known to the naive observers) was in the unadapted field. Each test trial was a 2AFC decision about which field appeared denser. Because each test trial was preceded by two adaptation pairs, the observer made a judgment about the third pair of textures presented on each trial. Duration and ISI parameters were the same as for adaptation. Responses were made via the keyboard.

Staircases terminated after eight turns with a terminal step-size of 5% of the standard density (i.e. 10 Gabor elements; initial step sizes were 20 Gabors and 15 Gabors prior to the first and second turns, respectively). PSEs were estimated by averaging the final six turns, and aftereffect size was expressed as natural logarithm of the ratio between the density (number of elements) in the adapted region and in the unadapted region at the PSE. For purposes of reference, an aftereffect size of 0.7 corresponds to a distortion in which a texture in the adapted region is matched to a texture in an unadapted region which is half as dense. An aftereffect size of 0 would correspond to subjectively matching objectively equal densities.

Results and discussion

Mean aftereffect sizes are plotted in Fig. 2 as a function of adapting spatial frequency, relative test orientation (same or different), and relative test spatial frequency (same or different). Individual observers' scores are shown in Table 1. These scores are collapsed across differences in phase because all of our analyses showed no effect of phase. In all analyses, test orientation, phase and spatial frequency are specified relative to the adapted orientation, phase and spatial frequency.

A $2 \times 2 \times 2 \times 2$ (adapted frequency $\times$ tested frequency $\times$ tested orientation $\times$ tested phase) repeated measures ANOVA revealed a reliable three-way interaction between adapted frequency, tested frequency and tested orientation $F(1,7) = 6.46$, $P < 0.05$. In separate analyses for different adaptation spatial frequencies, we found that adaptation to low-spatial frequency textures produced reliably lower aftereffects when measured with high-frequency Gabors ($M = 0.45$) than when measured with low-spatial-frequency textures ($M = 0.57$), $F(1,7) = 9.53$, $P < 0.05$. In contrast, after adaptation to high-spatial-frequency textures, the effect of test-texture size varied as

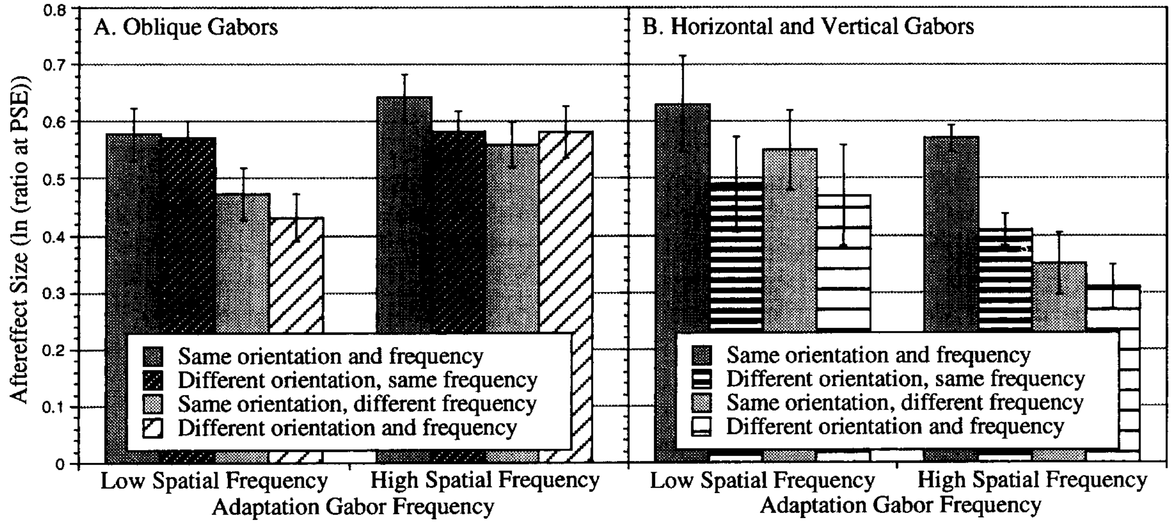

FIGURE 2. Results of Experiments 1A and 1B. Aftereffect size is plotted as a function of the spatial frequency of the adaptation stimulus. Texture type is defined relative to the adapting texture type. Error bars represent the standard errors of the means.

TABLE 1. Individual aftereffect scores for Experiment 1 (oblique orientations)

	Low spatial frequency adaptation				High spatial frequency adaptation			
	Same frequency test		Different frequency test		Same frequency test		Different frequency test	
	Same orientation	Different orientation	Same orientation	Different orientation	Same orientation	Different orientation	Same orientation	Different orientation
AH	0.27	0.44	0.27	0.23	0.43	0.56	0.43	0.57
FD	0.53	0.56	0.51	0.37	0.75	0.61	0.59	0.54
AM	0.91	0.65	0.65	0.61	0.90	0.74	0.80	0.72
NK	0.52	0.44	0.16	0.20	0.48	0.31	0.38	0.32
RC	0.51	0.52	0.58	0.48	0.53	0.48	0.38	0.35
RG	0.51	0.56	0.59	0.57	0.68	0.65	0.57	0.66
SG	0.60	0.58	0.45	0.38	0.56	0.54	0.58	0.63
SW	0.76	0.81	0.56	0.59	0.80	0.76	0.75	0.86
Avg	0.58	0.57	0.47	0.43	0.64	0.58	0.56	0.58

Each score is based on *ca* 40 trials in two staircases (averaged across differences in phase).

a function of orientation, $F(1,7) = 24.6$, $P < 0.01$: only when test textures were the same orientation as the adapting texture did same-size textures show greater aftereffects ($M = 0.64$) than different-sized textures ($M = 0.57$), $t(7) = 3.49$, $P < 0.025$.

The main conclusion supported by the data is that adaptation to low-spatial-frequency Gabors produced greater spatial-frequency specificity and less orientation specificity than did adaptation to high-frequency Gabors. Although the spatial-frequency shift account would have predicted density aftereffects in entirely the opposite direction (negative values) after adaptation to low spatial frequencies, the more greatly reduced aftereffects measured with high-frequency textures after adaptation to low-frequency textures could be interpreted as indicating some contamination from a spatial-frequency shift aftereffect. Given, however, that the same kind of specificity is present after adaptation to high-spatial-frequencies, a more parsimonious account is that the effects are simply somewhat specific to the adapting textures. This, and the orientation specificity found here for high-spatial-frequency Gabors, is consistent with existence of orientation specificity reported by Durgin and Proffitt (1996) insofar as the high-frequency Gabors are more segregated in the frequency domain than are the low-frequency Gabors used here.

EXPERIMENT 1B

One possible explanation for the minimal orientation specificity found in Experiment 1A is the oblique effect (Appelle, 1972; cf. also Foster & Ward, 1991). Oblique orientations are more difficult to discriminate than cardinal orientations and oblique orientations may be less well represented neurally. Consequently, we performed a non-oblique variant of Experiment 1A by tipping the monitor to one side by 45 deg so that the oblique screen orientations became cardinal orientations in the display (cf. Durgin & Wolfe, in press). The observers were two naive observers and the two authors. The methods were otherwise identical to Experiment 1A.

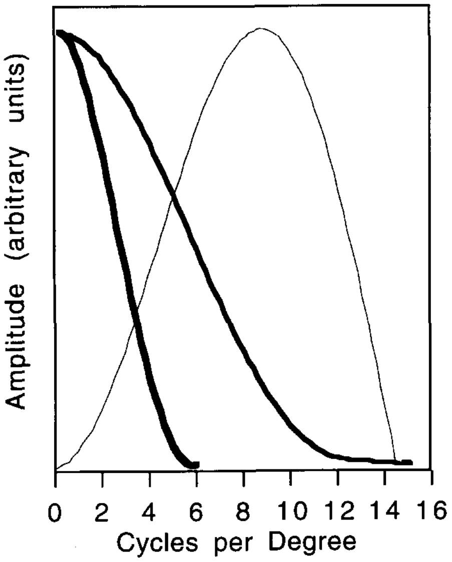

FIGURE 3. Results of Experiment 2. Aftereffect size for each kind of adaptation texture is plotted as a function of the tested texture. Error bars represent the standard errors of the means.

Results and discussion

Combined data for the four observers is plotted in Fig. 3, and individual data is shown in Table 2. Using cardinal rather than oblique orientations seems to have increased the importance of orientation information for the low-frequency adaptation textures relative to Experiment 1A with oblique textures. Instead of a three-way interaction, the $2 \times 2 \times 2 \times 2$ (adapted frequency × tested frequency × tested orientation × tested polarity) repeated measures analysis of aftereffect sizes revealed a more easily interpretable two-way interaction between tested orientation and tested frequency consistent with spatial-frequency specificity (not spatial-frequency shift), $F(1,3) = 14.4$, $P < 0.05$. The nature of this interaction can be expressed by a single straightforward conclusion that density aftereffects were strongest when both the orientation and the frequency of the test stimuli corresponded to those of the adaptation textures. This is in accord with the finding for high-spatial frequency adapting textures of Experiment 1A with oblique Gabors. Indeed, for high-spatial frequency adapting textures, the effect appears more highly pronounced with cardinal orientations than with obliquely oriented Gabors, and there are highly reliable effects of both test orientation, $F(1,3) = 110.8$, $P < 0.01$, and test size, $F(1,3) = 106.3$, $P < 0.01$, indicating stronger aftereffects when these properties matched the adaptation texture than when they did not.

The increased orientation specificity of the density aftereffect when cardinal rather than oblique orientations are used is consistent with the "oblique effect" (Appelle, 1972). This can be understood, for example, as a matter of preferential neural coding of cardinal orientations.

Because density-aftereffect size is modulated by similarity between adaptation and test textures (possibly in the frequency domain), some aspect of texture density aftereffects is clearly sensitive to the specific kind of texture used for adaptation (e.g. spatial frequency and orientation). However, there remains, in all cases, a strong component of aftereffect which appears to be independent of spatial frequency information.

EXPERIMENT 2

It might be objected that the range of spatial frequencies employed in Experiments 1A and 1B was small and that the question of size-specificity is therefore left open. This is especially important because the density aftereffect appears to be a kind of size aftereffect inasmuch as its perceptual effects include the apparent distortion of interdot distances. To better test the role of size or spatial-frequency information we varied texture element size (and spatial frequency). If density aftereffects were due entirely to spatial-frequency shift effects, then adaptation to high-spatial-frequency textures ought to produce density aftereffects (apparent reduction in perceived density) in low-spatial-frequency textures, however, adaptation to low-spatial-frequency textures ought to increase (or leave unaffected, if far enough removed in the frequency domain) the perceived density of high-spatial-frequency textures.

Method

The general apparatus and method was quite similar to that of Experiment 1A, except as noted below. Observers were the same two naive observers who participated in Experiment 1B and the two authors. Each observer

TABLE 2. Individual aftereffect scores for Experiment 1A (cardinal orientations)

	Low spatial frequency adaptation				High spatial frequency adaptation			
	Same frequency test		Different frequency test		Same frequency test		Different frequency test	
	Same orientation	Different orientation	Same orientation	Different orientation	Same orientation	Different orientation	Same orientation	Different orientation
AH	0.80	0.70	0.76	0.71	0.57	0.42	0.40	0.35
FD	0.58	0.49	0.52	0.42	0.62	0.45	0.39	0.29
CM	0.42	0.29	0.44	0.29	0.51	0.33	0.19	0.21
TW	0.72	0.47	0.49	0.46	0.59	0.45	0.43	0.39
Avg	0.63	0.49	0.55	0.47	0.57	0.41	0.35	0.31

Each score is based on approximately 40 trials in two staircases (averaged across differences in phase).

performed in three sessions of the experiment, and was adapted to a different kind of texture element each time. Staircases with each kind of texture element were used to measure density aftereffects in each session.

Textures. Three different texture elements were used. The smallest element was a square luminance-balanced dot (Carlson *et al*., 1984) constructed of a 4×4 center with a 1-pixel wide annulus of the opposite contrast against a gray background (average luminance of the dot was equal to the background gray). The peak spatial frequency of each dot was 8.8 c/deg. In the texture scattering process, exactly half of the dots in any given texture were white-centered and half were black-centered. In the balanced-dot textures, each dot was separated by at least 1 pixel-width of gray background from any other dot.

The other two kinds of element were Gaussian blobs with nominal diameters (defined as 4 standard deviations) of 7 pixels (0.14 deg) or of 15 pixels (0.3 deg). Textures composed of Gaussians were equally split between positive and negative luminance contrast so that all textures used had a "salt and pepper" appearance. Because balanced dots and the small Gaussian dots were of the same physical size for purposes of scattering texture elements, their densities could be matched directly (without overlap of elements). The dense adapting textures of these elements contained eight elements per square degree of visual angle, and the sparse textures contained one element per square degree of visual angle. For the larger Gaussian blobs, however, fewer dots could be scattered per unit of area without visible overlap. As a compromise between areal constraints and a desire to match absolute density, textures of large Gaussian blobs contained half as many elements (400) as did those of the smaller Gaussian dots. Because we are interested in comparing relative amounts of aftereffect between *tested* textures, differences in the densities of the adapting textures are acceptable.

Magnitude spectra of the three types are dot are shown in Fig. 4. The texture presentation regions were reduced to 8.75×12 deg (437×600 pixels) rectangles to the left and right of fixation because the high-spatial-frequency balanced dots were difficult to see in the farther periphery. Texture presentations times were identical to those in Experiment 1.

Adaptation and measurement. In each experimental session there was an initial period of adaptation (120 presentations) and then twelve measurement staircases were interleaved. The format of the staircases was just like that of Experiment 1, and two readaptation stimuli were presented before each trial. Each texture type was measured by four staircase sequences. In each case, the density presented in the adapted region was either half or a third of the adapting density. PSEs in the unadapted region were determined for these densities. (Densities for large Gaussian blobs differed from the others by a factor of two, as mentioned above.) Each session lasted about half an hour and included *ca* 220 trials.

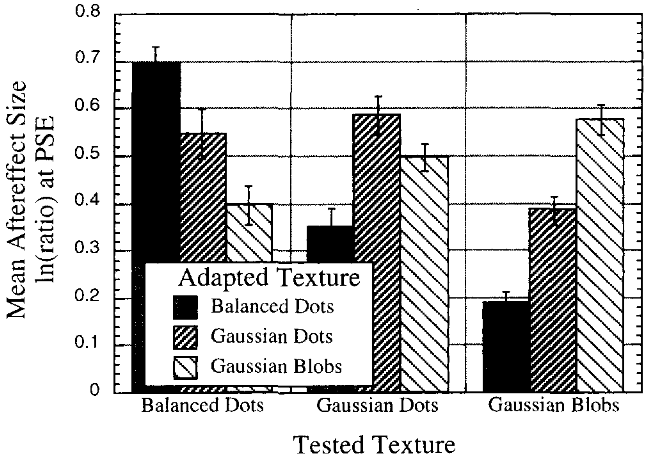

FIGURE 4. Magnitude spectra of texture stimuli used in Experiment 2. Spectra are shown for balanced dot elements (thin line), narrow gaussian blobs (medium line), and broad Gaussian blobs (thick line).

Results and discussion

PSEs computed from each staircase were converted to logarithms of their ratios and subjected to a $3 \times 3 \times 2$ (adapting texture $\times$ test texture $\times$ test density) repeated measures ANOVA. As expected from spatial-frequency specificity demonstrated in Experiments 1A and 1B, the aftereffect size measured with a particular kind of texture differed as a function of the kind of adapting texture $F(4,12) = 31.47$, $P < 0.01$. As illustrated in Fig. 3, aftereffect strength as measured with a particular texture is greatest when that same texture was used for adaptation, and the amount of aftereffect appears related to the similarity in size of the adapting and test textures. Mean aftereffect sizes for individual observers are shown in Table 3.

TABLE 3. Individual aftereffect scores for Experiment 2

	Balanced dot adaptation			Gaussian dot adaptation			Gaussian blob adaptation		
	Balanced dots	Gaussian dots	Gaussian blobs	Balanced dots	Gaussian dots	Gaussian blobs	Balanced dots	Gaussian dots	Gaussian blobs
AH	0.83 ± 0.03	0.48 ± 0.03	0.22 ± 0.01	0.84 ± 0.02	0.82 ± 0.04	0.48 ± 0.05	0.52 ± 0.04	0.61 ± 0.02	0.55 ± 0.04
FD	0.65 ± 0.02	0.19 ± 0.06	0.21 ± 0.04	0.32 ± 0.02	0.51 ± 0.02	0.44 ± 0.02	0.38 ± 0.04	0.38 ± 0.04	0.61 ± 0.03
CM	0.56 ± 0.05	0.25 ± 0.03	0.08 ± 0.02	0.48 ± 0.06	0.52 ± 0.07	0.29 ± 0.04	0.18 ± 0.05	0.47 ± 0.04	0.44 ± 0.06
TW	0.76 ± 0.05	0.48 ± 0.06	0.25 ± 0.02	0.54 ± 0.04	0.48 ± 0.05	0.34 ± 0.07	0.51 ± 0.05	0.53 ± 0.06	0.71 ± 0.06

Each score is based on *ca* 80 trials in four staircases (averaged across differences in density). Error terms represent standard errors of the mean.

Two facts about the present data are indicative of a weakness of the spatial-frequency shift account of density aftereffects. First, whether adapting to large Gaussian blobs or to high-spatial-frequency balanced dots, the density aftereffect measured here is always a reduction in perceived density in the adapted region. In other words, the *direction* of adaptation appears to be independent of the relative spatial frequencies of the adaptation and test textures. Indeed, the effect shows a remarkable level of transfer between textures with very different Fourier spectra.

On the other hand, the *magnitude* of aftereffect appears to be directly related to the similarity between the adaptation and test textures. This implies that there is a filter-specific aspect of density adaptation and density coding.

EXPERIMENT 3

The textures examined in Experiments 1 and 2 were carefully constructed so that density could be manipulated independently of element size, but in most circumstances, size and density covary. For many normal visual textures there is no clear "element". Natural textures are continuous. The earlier experiments in this paper have demonstrated that the perceptual distortion of texture density which we refer to as a texture density aftereffect cannot be explained in terms of a spatial-frequency shift aftereffect. However, the textures employed were all composed of discrete elements of uniform size. For such textures, size information is not important to the evaluation of density. In the present experiment we continued to adapt observers to artificial textures of matched spatial frequency, but we assessed the perceptual distortion of texture density using naturalistic visual textures for which density and spatial frequency covary. To avoid concern that our adaptation textures were higher in spatial frequency than our test textures, we used large Gaussian blobs as adaptation texture elements, thus minimizing the adaptation of high-spatial-frequency information.

Method

Design. In order to determine whether naturalistic textures would be susceptible to aftereffects of density (rather than spatial frequency exclusively), we determined PSEs between naturalistic textures presented in two parts of the visual field before and after one of those fields was adapted to dense Gaussian-blob textures. In pre-adaptation sessions, observers made 10 2AFC comparisons of each of the 42 combinations of seven different magnifications for each of four texture types, totaling 1680 judgments per observer. The same number of texture judgments were again performed after the observer was adapted to dense textures. Texture comparisons were presented in blocks of 210 trials of a single texture type (five repetitions of the complete set of 42) and the order of doing different types was varied between observers.

Observers. The two authors and two naive observers (one college undergraduate and one high-school student) participated. The naive observers were laboratory assistants who were unfamiliar with the specific goals of the experiment.

Apparatus and display. The experiment was conducted using a Power Macintosh 9500/120, with a ViewSonic 21PS multisync monitor (set to 1152×870 pixels with vertical refresh of 75 Hz) as the display. At the viewing distance of 54 cm, the resolution of the monitor was 29 pixels per degree of visual angle. The display regions were 240×320 pixels (8×10.7 deg) and positioned just to the left and right of a central fixation mark. The mean luminance of the display was 54 cd/m^2, and it was viewed in a dimly lit room. Response was made by keyboard.

Textures. Four different types of texture were used as representative "naturalistic textures". The four types are shown in Fig. 5 and will be referred to as clouds, wood, liquid and granite. These textures were all developed using Adobe TextureMaker 1.0. These four were chosen because they covered a range of sizes and were variable with respect to the distinctness of the elements of which they are composed. Seven different densities of each texture type were created. In two cases (liquid, clouds) we used built-in magnification control in the texture rendering program. For the other two (wood, granite), scaling was obtained by generating large images of equal-density textures that could then be digitally minified and cropped to final size. The most extreme magnifications differed from each other by a linear factor of 1.5 (size), which is a square factor of 2.25 (density). The textures shown in Fig. 5(a) are 192×192-pixel croppings from the middle magnification. A similarly sized "artificial" Gaussian blob texture is shown in Fig. 5(b). Full texture size was 240×320 pixels in all cases. Natural texture presentation duration was 400 msec on each trial.

Adaptation. The adapting textures were generated as in Experiment 2, from dark and light Gaussian blob elements which meant that spatial frequency information was still held fixed (uncorrelated with density) during adaptation. In this experiment, the blob size (defined by a radius of 2 standard deviations) was 10 pixels in diameter which was equivalent in visual angle to the largest blobs of Experiment 2. The high-density adapting texture was densely packed with *ca* 430 elements (fewer when space could not be found for all), and the low-density texture contained 60 scattered blobs. To promote a strong aftereffect, adaptation consisted of both an initial adaptation phase of 64 presentations (1000 msec per display), as well as a measurement period of four staircases with two readaptation stimuli presented before each trial. This adaptation and measurement period lasted *ca* 10 min. During the post-adaptation naturalistic-texture measurement sessions, two readaptation texture pairs were presented before each test trial to maintain texture density adaptation.

Measurement and analysis. Choice probabilities between different texture magnifications (pooling across similar differences in magnification) were converted to *z*-

(a)

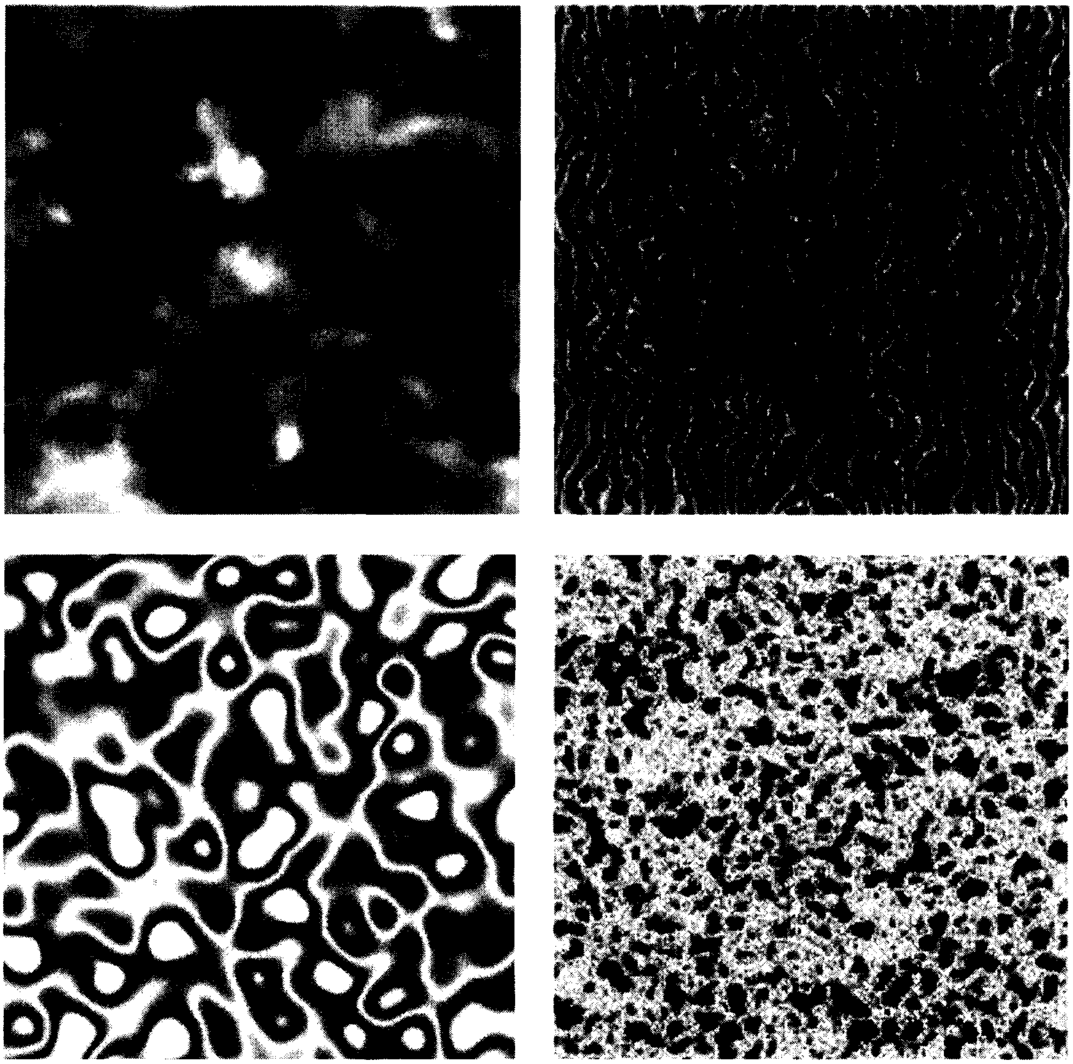

(b)

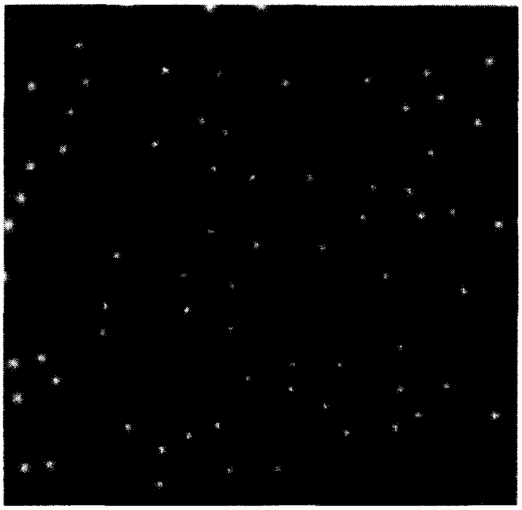

FIGURE 5. (a) Sample textures used in Experiment 3. The textures shown here are from the intermediate magnification level. Clockwise from the upper left are clouds, wood, granite and liquid. Each sample is a 192×192 pixel piece from the original 320×240 texture. (b) Sample medium density texture of elements used as adaptation elements. Sample is same size as those shown in Fig. 3(a).

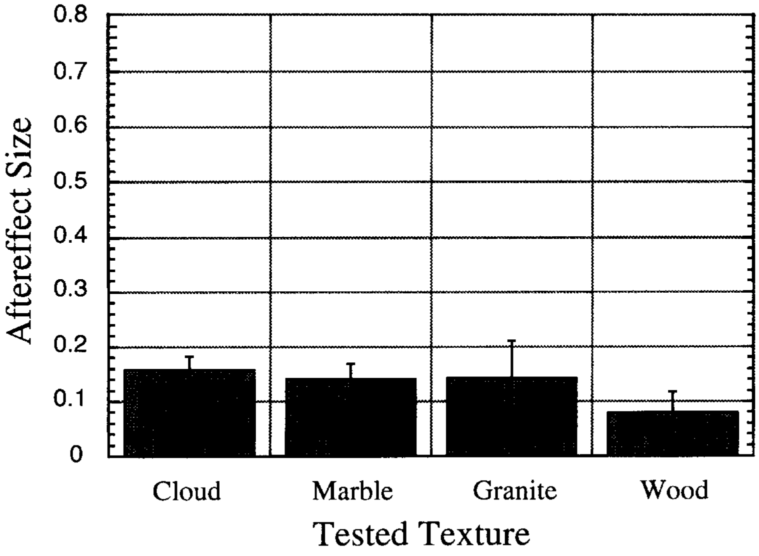

FIGURE 6. Results of Experiment 3. Aftereffect size at PSE was computed for each observer for each texture type based on choice probabilities before and after adaptation. Means are shown here, with standard error bars. See text for details.

scores, and logarithms of texture density ratios at their PSE were computed for before and after adaptation for each texture type.

Results and discussion

For easy comparison with earlier figures, the mean log(ratio) values expressing the difference between the post-adaptation measurement and the pre-adaptation measurement are shown in Fig. 6. Because the present analysis was designed primarily to detect the existence of a density aftereffect, rather than to compare aftereffect strengths among textures, the PSEs computed for each observer were analyzed in a 2×4 (adaptation state $\times$ texture type) repeated-measures ANOVA. As predicted, the log(ratio) PSEs while adapted ($M = 1.33$) were reliably greater than those measured prior to adaptation ($M = 0.008$), $F(1,3) = 25.5$, $P < 0.05$. The analysis failed to find any reliable effect of texture type, $F(3,9) = 1.54$, NS. Nor was there evidence for a reliable interaction between texture type and adaptation, $F(3,9) < 1$.

It is evident by comparison of Fig. 6 with Figs 2 and 3 that the amount of aftereffect measured in Experiment 3 is smaller than that measured in the preceding experiments. This reduction in measured distortion may result both from the differences between the adaptation and test textures, and from the fact that in this experiment alone did there exist informative spatial frequency differences between test textures that were objectively unequal in density. (Note that the adaptation texture remained neutral with respect to spatial frequency, though the test textures did not.) If observers used unadapted spatial frequency information to help make texture comparisons, the result would be an underestimation of the true extent of density adaptation.

Overall, these results support the hypothesis that density aftereffects extend to a variety of naturalistic textures. Although there is nothing in this data that contradicts Anstis (1974) findings that spatial-frequency aftereffects can be obtained with naturalistic textures, these results indicate that there are some kinds of texture aftereffects measurable with naturalistic textures that are not spatial-frequency shift aftereffects.

GENERAL DISCUSSION

What does the texture density aftereffect tell us about the visual representation of texture? To answer this question we must give an account of two levels at which texture representation can be construed. At the level of phenomenal awareness, the aftereffect of texture density is experienced as a reduction in the number of elements, but also as an increase in inter-element spacing. In this sense, texture density is a visual variable that characterizes the distribution of texture in space. At a second level, that of visual representation, however, the aftereffect suggests that density is coded as a one-dimensional value, a scalar, because the aftereffect is unidirectional. Unlike spatial-frequency shift aftereffects, there is no directional shift away from the adapted value. Moreover, although one could imagine that it was coded as the amplitude of local texture analyzer activity [but see Durgin (1996a)], such an account would seem to suggest that one ought to simultaneously get spatial frequency shifts as well. To the extent that density aftereffects seem to transfer between texture types, it would seem that density is represented at a later (or parallel) stage of visual analysis that pools across element types.

Because texture density seems to be relatively independent of Fourier representation, one plausible interpretation is that it occurs in a second-order stage of analysis (e.g. Sperling, 1989) via a representation of contrast energy. Durgin (1996b) has shown that aftereffects to differences in texture contrast are independent of those to differences in texture density (e.g. contrast aftereffects are monocular). However, it may be that once peripheral (local) contrast differences are eliminated, then global contrast differences (e.g. resulting from differences in texture density) may be used to represent texture distribution across a range of different element types. It should be emphasized here that Fourier analysis does not help to extract statistics about spacing in the face of random processes, so rectification processes are simply inadequate to make density into a easily managed Fourier dimension in the way that some other second-order effects can be understood as the result of rectification followed by a second spatial frequency analysis.

The perceptual representation of visual texture is an abstraction of information, not an image, nor even the Fourier transform of an image. In the present series of experiments, we have provided evidence that the abstraction includes a dimension of density that is distinct from traditional spatial frequency, though it may be encoded in a way that is somewhat specific to various texture properties. This dimension seems to apply to a broad range of textures, artificial and naturalistic, which can be said to have abstract or concrete elemental units.

We suggest that density representation [and the representation of the variance of density in a texture—see Durgin (1995)] may be considered a way of coding spatial information about the distribution of texture in a non-spatial format. That is, although density is more-or-less locally represented across space (cf. Durgin & Cole, 1997), the exact positions of individual elements are not, since their spatial distribution is apparently represented by summary statistics. Ultimately, if texture segregation algorithms provide visual access to texture features, it may nonetheless be inadequate to simply attach those features to "maps" in the brain. Instead, information about the spatial distribution of texture might be coded by such variables as "density" that convert spatially-interepretable information into scalar intensity values. When the mechanisms underlying these values get adapted, the effect produces a subjective impression of the local mutual repulsion of texture elements.

REFERENCES

Anstis, S. M. (1974). Size adaptation to visual texture and print: Evidence for spatial-frequency analysis. *American Journal of Psychology, 87*, 261–267.

Appelle, S. (1972). Perception and discrimination as a function of stimulus orientation: The "oblique effect" in man and animals. *Psychological Bulletin, 78*, 266–278.

Blakemore, C. & Campbell, F. W. (1969). On the existence of neurones in the human visual system selectively sensitive to the orientation and size of retinal images. *Journal of Physiology, 203*, 237–260.

Blakemore, C. & Sutton, P. (1969). Size adaptation: A new aftereffect. *Science, 166*, 245–247.

Carlson, C. R., Moeller, J. R. & Anderson, C. H. (1984). Visual illusions without low spatial frequencies. *Vision Research, 24*, 1407–1413.

Durgin, F. H. (1995). Texture density adaptation and the perceived numerosity and distribution of texture. *Journal of Experimental Psychology: Human Perception and Performance, 21*, 149–169.

Durgin, F. H. (1996a). Luminance-contrast adaptation and density adaptation: Two second-order texture aftereffects and their interactions. *Investigative Ophthalmology & Visual Science, 37*, S292.

Durgin, F. H. (1996b). Visual aftereffect of texture density contingent on color of frame. *Perception & Psychophysics, 58*, 207–233.

Durgin, F. H. & Cole, R. (1997). Texture-density aftereffects to filled-in and suppressed portions of textures. *Investigative Ophthalmology & Visual Science, 38*, S636.

Durgin, F. H. & Proffitt, D. R. (1991). Detection of texture density: Evidence from adaptation. Paper presented at the Annual Meeting of the Psychonomic Society, San Francisco, November, 1991.

Durgin, F. H. & Proffitt, D. R. (1996). Visual learning in the perception of texture: Simple and contingent aftereffects of texture density. *Spatial Vision, 9*, 423–474.

Durgin, F. H. & Wolfe, S. E. (1997). Global precedence in visual search? Not so fast: Evidence instead for an oblique effect. *Perception, 26*, 321–332.

Foster, D. H. & Ward, P. A. (1991). Asymmetries in oriented-line detection indicate two orthogonal filters in early vision. *Proceedings of the Royal Society (London B), 243*, 75–81.

Gibson, J. J. (1933). Adaptation, after-effect, and contrast in the perception of curved lines. *Journal of Experimental Psychology, 16*, 1–31.

Gilden, D. L., Bertenthal, B. I. & Othman, S. (1990). Image statistics and the perception of apparent motion. *Journal of Experimental Psychology: Human Perception and Performance, 16*, 693–705.

Graham, N. V. S. (1989). *Visual pattern analyzers*. New York: Oxford University Press.

Köhler, W. & Wallach, H. (1944). Figural aftereffects: An investigation of visual processes. *Proceedings of the American Philosophical Society, 88*, 159–201.

MacKay, D. M. (1964). Central adaptation in mechanisms of form vision. *Nature, 203*, 993–994.

Sperling, G. (1989). Three stages and two systems of visual processing. *Spatial Vision, 4*, 183–207.

Walker, J. (1966). Textural aftereffects: Tactual and visual. Unpublished doctoral dissertation. Boulder, CO: University of Colorado.

Acknowledgements—This research was supported by the Howard Hughes Medical Institute and a faculty research grant from Swarthmore College. We wish to thank Charity Miller, Colleen Milligan and Tori Washington for help with data collection and analysis. Portions of this article were based on a Senior Honor's Thesis at Swarthmore College by Alexander C. Huk, who is now at the Department of Psychology, Stanford University.